JACS
JOURNAL OF THE AMERICAN CHEMICAL SOCIETY

ARTICLE

pubs.acs.org/JACS

Soft- and Reactive-Landing of Cr(aniline)$_2$ Sandwich Complexes onto Self-Assembled Monolayers: Separation between Functional and Binding Sites

Shuhei Nagaoka,[†] Kaori Ikemoto,[†] Kazuki Horiuchi,[†] and Atsushi Nakajima*[,†,‡]

[†]Department of Chemistry, Faculty of Science and Technology, Keio University, 3-14-1 Hiyoshi, Kohoku-ku, Yokohama 223-8522, Japan

[‡]ERATO, Japan Science and Technology Agency, 3-2-1 Sakado, Takatsu-ku, Kawasaki 213-0012, Japan

Supporting Information

ABSTRACT:

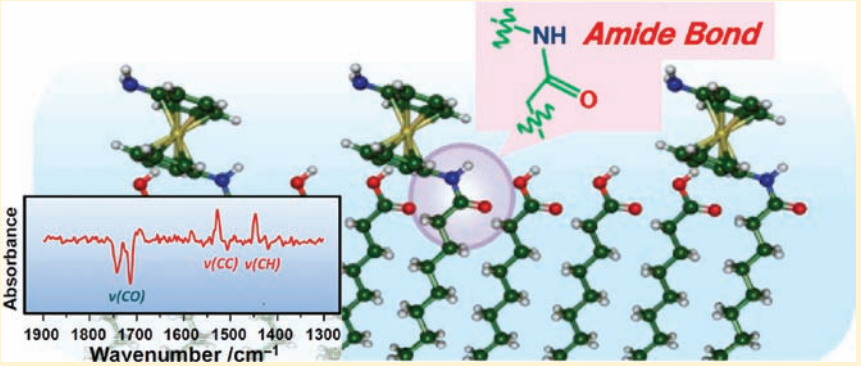

Soft- and reactive-landing of gas-phase synthesized cationic Cr(aniline)$_2$ complexes onto self-assembled monolayers of methyl-terminated (CH_3−SAM) and carboxyl-terminated (COOH−SAM) organothiolates coated on gold were performed at hyperthermal collision energy (5−20 eV). The properties of the Cr(aniline)$_2$ complexes on the SAM surfaces were characterized using infrared reflection absorption spectroscopy (IRAS) and temperature-programmed desorption (TPD), together with theoretical calculations based on density functional theory (DFT). For the CH_3−SAM, the Cr(aniline)$_2$ complexes were embedded inside the SAM matrix in a neutral charge state, keeping a sandwich structure. For the COOH−SAM, the IRAS and TPD study revealed that the amine-containing Cr(aniline)$_2$ complexes were bound to the SAM surface in two forms of physisorption and chemical linking through an amide bond. In the desorption, the latter form appeared as the reaction product between organothiolates and Cr(aniline)$_2$ above 400 K, where the organothiolate molecules, forming the SAM, were desorbed from the gold surface. The results show that the hyperthermal depositions onto a COOH−SAM bring about reactive-landing followed by covalent linking of an amide bond between the amine-containing Cr(aniline)$_2$ complexes to the carboxyl-terminated SAM surface, in which the binding sites can be separated from the functional sites of the d−π interaction.

1. INTRODUCTION

The research field of size-selected clusters originated from the development of mass-selected cluster beam techniques in the early 1980s.[1−6] As well as pure clusters consisting of single elements, furthermore, gas-phase cluster synthesis provides a chemical advantage for producing novel composite clusters of alloy, ionic, and organometallic clusters. Over the past decade, in particular, the combination of laser-vaporization and molecular beam methods has yielded various kinds of clusters and organometallic complexes in the gas phase,[7−14] and the one-dimensional (1D) organometallics exhibit unique size-dependent electronic and magnetic properties, originating from the d−π interaction between a transition metal atom and organic ligands in the 1D anisotropic structures.[13−19]

The notion that the novel properties of these functional gas-phase species might be utilized to create advanced functional nanomaterials leads to a strong motivation to decorate surfaces with gas-phase compounds such as clusters[20−32] and biomolecules[33−38] and also to assemble designer nanostructured materials from them. An important theme to this research effort is to establish a well-controlled way to produce novel nanostructured surface based on an understanding of the interaction between the compounds and surface.[39,40]

In the previous studies of cluster-deposition experiments conducted in ultrahigh vacuum,[21,41,42] the method to preserve

Received: June 10, 2011
Published: October 27, 2011

the clusters size demonstrated the soft-landing of clusters onto cryogenically cooled surfaces covered with a rare-gas matrix, which inhibits cluster diffusion along with efficient energy dissipation of collision energy at the deposition.[20,21] To prevent thermal diffusion of the clusters at room temperatures and above, it is necessary to fix the cluster more tightly to the surface, and two techniques used to produce size-selected cluster arrays of arbitrary density are known as (1) the use of surface defects created before cluster deposition[43−45] and (2) self-pinning of clusters, in which the clusters are pinned to the surface where they land above a critical threshold impact energy.[31,32] Indeed, these two ways are good for the preservation of cluster size, but the clusters encounter considerable structural deformation through cluster−surface interactions. Thus, to realize nanostructured functional surface decorated with organometallic clusters, the preservation of the free organometallics' properties,[46,47] especially the functional d−π interaction sites, on a surface is a key issue in deposition studies; ideally the cluster should possess two different sites for the functionality and the binding, because the binding required to fix the clusters at surfaces would generally cause a serious change in the clusters' characteristic gas-phase properties. From the viewpoint of the separation of the binding and functional d−π sites of the complexes, it seems suggestive to immobilize gas-phase peptide ions onto organic surfaces through the covalent bonding between the peptide's "residual" (not skeletal) group and terminal group of the surface.[35]

Self-assembled monolayers (SAMs) of organic molecules formed on metal and semiconductor surfaces are an excellent deposition target for the soft-landing[48−50] because the long-chain alkanethiolate SAM effectively dissipates the translational energy of the projectiles.[51,52] Our previous works have demonstrated that the organometallic complexes are embedded in the SAM, as a result of their soft-landing at hyperthermal collision energy of ∼20 eV. The embedded complexes can be trapped just above room temperature (up to around 300 K with C_{22}−SAM) with negligible deformation, where the ordering of the alkyl-chains provides two-dimensional solid-like surroundings.[53,54] Furthermore, chemical modification of organic molecules forming SAM matrices can produce a wide variety of adsorption regime and/or supporting system of gas-phase species soft-landed on the SAM substrate.[55−60] In particular, terminal modification of the SAM surface can be used to change the fixation position of the organometallic complexes; in *n*-alkanethiol (CH_3−SAM), complexes are embedded inside the SAM, while in a carboxyl-terminated SAM (COOH−SAM), they are fixed at the top of surface of the SAM because the rigid hydrogen-bonding networks formed at the carboxyl-terminated surface inhibit the penetration of the incoming clusters inside the SAM.[59]

In this work, we have developed a new method to fix the organometallic complexes on a surface with the separation of the binding and functional d−π sites of the complexes to achieve the preservation of the organometallics' properties above room temperatures. Together with terminal modification of the SAM surface from methyl to carboxyl group, aromatic ligands of the organometallic complex are chemically modified; the derivatives of M_1(benzene)$_2$ substituted by amine groups, a Cr_1(aniline)$_2$ complex, were deposited onto COOH−SAM to perform the immobilization with covalent linking between the complexes and the SAM surface. The resulting adsorption properties of the soft-landed complexes were investigated by means of infrared reflection absorption spectroscopy (IRAS), temperature programmed desorption (TPD) measurements, and harmonic frequency analyses based on density functional theory (DFT). Reactive-landing of the Cr(aniline)$_2$ complexes on COOH−SAM was achieved through a formation of an amide bond, demonstrating that the chemical modifications of both the terminal group of the SAM and the aromatic ligands of organometallic clusters enable us to fix the functional complexes on the surface far above room temperatures of ∼380 K, where binding sites are separated from functional sites.

2. EXPERIMENTAL AND COMPUTATIONAL SECTION

Details of experimental procedures and setup have been described elsewhere.[53] A commercially available 10 × 10 mm gold substrate, Au (100 nm thickness)/Ti/silica (PREX Sheet K, Tanaka Precious Metals), was used as the gold surface. To remove organic contaminants from the gold surface, the substrate was chemically cleaned by dipping in a piranha solution (3:1 concentrated H_2SO_4−H_2O_2) for about 20 min. The gold substrate was subsequently immersed into a 0.5 mM ethanolic solution of 1-octadecanethiol and 16-carboxypentadecanethiols containing 2% (v/v) trifluoroacetic acid at ambient temperature for about 20 h to form methyl-terminated SAMs (C_{18}−SAM; hereafter cited as CH_3−SAM) and carboxyl-terminated SAMs (COOH−SAM).[46] After the formation of the SAMs, the substrates were treated by rinsing with neat ethanol, and then the COOH−SAMs only were additionally rinsed with a 10% (v/v) ethanolic solution of aqueous ammonia (28−30%) several times. The formations of the SAM substrates thus obtained were characterized by means of infrared reflection absorption spectroscopy (IRAS) under vacuum condition (∼1.5 Torr) using an FT-IR spectrometer (IFS66 vi, Bruker Optics).

Chromium (Cr)−aniline complexes are produced in a molecular beam by the reaction of laser vaporized Cr atoms with aniline vapor. Cationic complexes are extracted by a quadrupole deflector, and only the Cr(aniline)$_2$ complexes are mass-selected by a quadrupole mass spectrometer (150QC, Extrel), respectively. These cations are subsequently deposited onto the SAM substrate mounted in an ultrahigh vacuum chamber (∼2 × 10^{-10} Torr). The temperature of the substrate can be cooled to 150 K by a liquid nitrogen cryostat, with the peak kinetic energies of ∼5−20 eV. The cation beam was focused onto the substrate by use of electrostatic lenses, within the size of <10 mmϕ, and the total amount of the deposited cations was determined by integrating the ion current (typically 4−6 nA) on the substrate during the deposition of the complexes.

The IRAS spectra for the deposited complexes were obtained with IR at an incident angle of ∼80° with respect to the surface normal, and the spectra were recorded with the a resolution of 2 cm^{-1}. The TPD measurements were carried out with a heating rate of 1−3 K/s after the deposition of the complexes, and the desorption species were detected by another quadrupole mass spectrometer (150QC, Extrel) via electron impact ionization (∼70 eV).

Geometry optimizations and harmonic frequency analyses for the Cr−aniline complexes were carried out using density functional theory (DFT) with the Gaussian 03 quantum chemistry programs.[61] Our previous studies on vibrational frequency analysis for organometallic complexes of first-row transition metals and π-donor ligands concluded that the B3LYP functional provides realistic correspondence with the experimental IR results.[62−64] Accordingly, all of the calculations described here used the B3LYP functional, with a scaling factor of 0.967 applied to the computed harmonic vibrational frequencies using values from the experimental IR spectrum for aniline vapor.[64] The TZVP basis (polarization functions) was used for the Cr center, and the split valence triple-ζ 6-311+G(d,p) basis (polarization for all, diffuse functions for all but H) was used for the rest of the atoms.

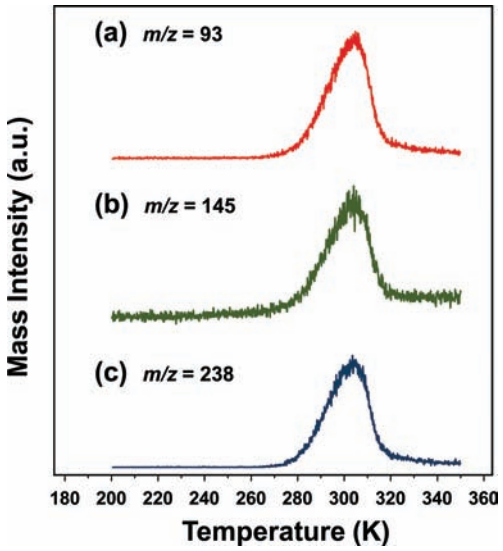

Figure 1. TPD spectra obtained for $Cr(aniline)_2$ complexes soft-landed on CH_3−SAM after deposition of 5×10^{13} cations at the surface temperature of 200 K with the heating rate of 1 K/s. Three kinds of desorption mass signals were mainly recorded: (a) aniline (93 amu), (b) Cr(aniline) (145 amu), and (c) $Cr(aniline)_2$ (238 amu).

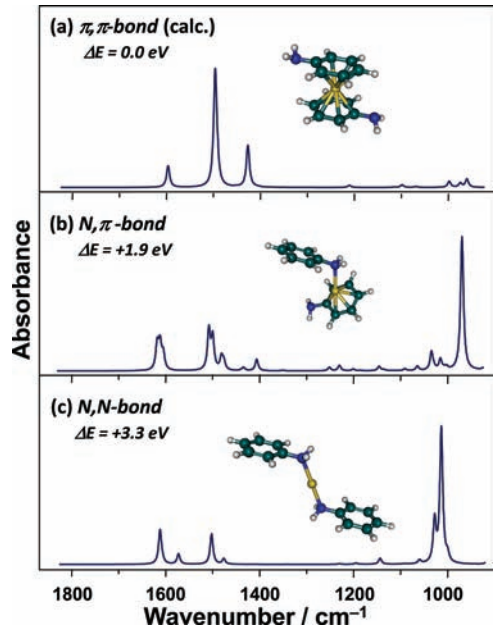

Figure 2. Theoretically simulated IR absorption spectra for $Cr(aniline)_2$ complexes in three possible conformations based on metal−π and metal−N bonding: (a) π,π-bond, (b) N,π-bond, and (c) N,N-bond, where the bandwidth of 10 cm^{-1} is given for each band.

3. RESULTS AND DISCUSSION

3.1. Soft-Landing of $Cr(aniline)_2$ on CH_3−SAM. The geometric structure of gas-phase-synthesized $Cr(aniline)_2$ complexes was investigated through soft-landing isolation technique using the CH_3−SAM as a matrix. First, the desorption behaviors of the complexes were examined with TPD measurements after the hyperthermal depositions (20 eV). Figure 1 shows the TPD spectra for species desorbed from the CH_3−SAM substrate after the soft-landing of $Cr(aniline)_2$ cations (m/z = 238) at the surface temperature of 200 K. The desorption signals were observed for the parent $Cr(aniline)_2$ (m/z = 238) along with the species of Cr(aniline) (m/z = 145) and aniline (m/z = 93). As seen in Figure 1, the thermal desorption starts at ∼280 K and the desorption rates reach maxima at ∼305 K, and then rapidly decrease, indicating a first-order desorption profile,[65] corresponding to the desorption of embedded $Cr(aniline)_2$ inside the CH_3−SAM matrix.[53,58] All three desorption signals, moreover, illustrate identical peak profiles, showing that the latter two of Cr(aniline) and aniline are fragments of $Cr(aniline)_2$ produced through the electron-impact ionization in the mass spectrometer. Furthermore, because no TPD signals could be obtained without the electron-impact ionizer, it is confirmed that $Cr(aniline)_2$ cations deposited were neutralized on the substrate, keeping their chemical composition in the SAM matrix even after the hyperthermal collision event.

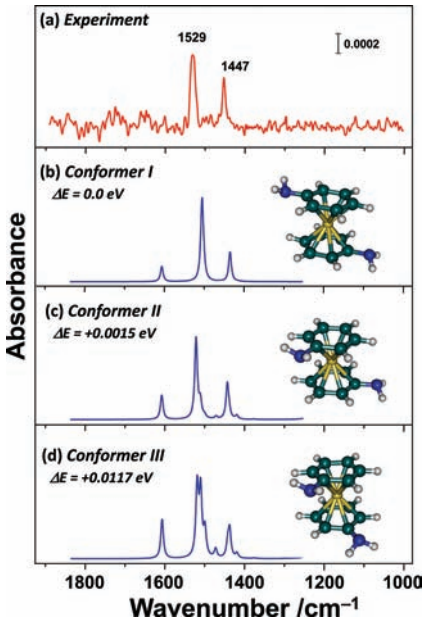

Figure 3. IRAS spectra for $Cr(aniline)_2$ complexes soft-landed on CH_3−SAM after deposition of 1.5×10^{14} cations at the surface temperature of 200 K, along with simulated IR spectra for sandwich formed $Cr(aniline)_2$ complexes in three rotational conformations, where the bandwidth of 10 cm^{-1} is given for each band in the simulated spectra.

For the complex of transition metals and aniline molecules, the aniline ligand provides two possible sites of the π-ring and amino-group for metal atom attachment, which generate metal−π and metal−N bonds, respectively.[64] As representative isomers, three kinds of isomers are conceivable: π,π-bond, N,π-bond, and N,N-bond, as shown in Figure 2. Among them, a sandwich isomer (π,π-bond in Figure 2a) through the interaction between a metal atom and π-ring isomer is energetically 1.9 and 3.3 eV more stable than the other two isomers in Figure 2b and c with single and double N-bond isomers. Furthermore, the structures optimized by the DFT calculations allow us to simulate their IR spectra, and the three isomers actually exhibit different absorption profiles, as shown in Figure 2. When a transition metal atom binds to an aniline molecule at the NH_2 group (N-bond), the simulated IR spectra illustrate intense absorption bands around 1000−1100 cm^{-1}, originating from the frustrated inversion mode of the NH_2 group. The calculation results clearly show

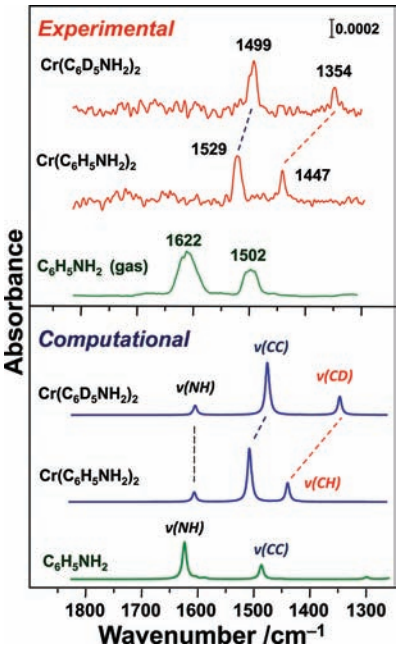

Figure 4. IRAS spectra and simulated IR absorption spectra for deuterated-Cr(aniline)$_2$ complexes together with their undeuterated spectra as references. Gas-phase IR data[76] and simulated IR spectra for a free aniline molecule are also displayed as references.

that each spectral feature can identify either the π-bond or the N-bond structures for the Cr(aniline)$_2$ complexes by comparison with the experimental IRAS measurements.

Figure 3 shows an experimental IRAS spectrum after the soft-landing of 1.5×10^{14} Cr(aniline)$_2$ cation beam onto the CH_3−SAM with the collision energy of ~20 eV at the surface temperature of 200 K. Two absorption bands appeared at 1447 and 1529 cm^{-1}, and no prominent IR bands appear around 1000−1100 cm^{-1}, which are characteristic of N,π-bond and N, N-bond isomers in Figure 2b and c. Therefore, the structures of the Cr(aniline)$_2$ complexes landed can be presumed to take a sandwich structure of π,π-bond in Figure 2a, which is consistent with our DFT calculation mentioned. In addition, a gas-phase study with IR spectroscopy has indeed revealed a sandwich form of cationic Cr(aniline)$_2$ complexes.[64]

It is noted that the IR bands observed exhibit relatively broad bandwidth of ~15 cm^{-1} (full-width at half-maximum). In the IR spectrum of Cr(benzene)$_2$, for comparison, the IR peaks typically exhibit the bandwidth of ~4 cm^{-1},[59] and then the broad IR peak implies that a number of Cr(aniline)$_2$ conformers having different rotational angles between NH_2 groups might contribute to the band envelopes. Figure 3 further shows the simulated IR spectra for Cr(aniline)$_2$ for three representative conformers having different rotational angles of two ligands. The energies of the rotational conformers are almost equal within ~0.01 eV in the DFT calculations, and the rotational barrier estimated was only ~0.03 eV, which is small enough to pose free rotation of two ligands at the temperature of 200 K. Because the vibrational bands of the rotational conformers exhibit slightly different frequencies as shown in Figure 3, the broad bandwidths for Cr(aniline)$_2$ might be attributed to the mixing of the rotational conformers.

The calculated spectra represent three noticeable absorption bands in the region of 1300−1800 cm^{-1} for all of the conformers. The absorption bands originate from NH bending vibrations (ν(NH), 1600 cm^{-1}), in-plane ring CC stretching/deforming vibrations (ν(CC), 1500 cm^{-1}), and in-plane CH bending vibrations (ν(CH), 1430 cm^{-1}), respectively. However, our experimental IR spectra exhibit only two notable absorption signals. To ascertain the vibrational assignments for the landed Cr(aniline)$_2$, the deuteration effects of aniline ligands on the IR absorption frequencies were investigated.

Figure 4 shows the IRAS spectrum for Cr($C_6D_5NH_2$)$_2$ containing deuterium-substituted aniline: Cr($C_6D_5NH_2$)$_2$ supported on the CH_3−SAM substrate after the deposition of 2×10^{14} ions at the surface temperature of 200 K, together with that of former undeuterated one of Cr($C_6H_5NH_2$)$_2$ as a reference. Calculated IR spectra for the deuterated and undeuterated complexes (conformer I) are also displayed in the lower trace. For the experimental spectra of Cr($C_6D_5NH_2$)$_2$ complexes, the two IR peaks were observed at 1499 and 1354 cm^{-1}. The peak frequencies were predictably red-shifted due to the deuterium substitution. Judging from the similarity in relative peak intensities, the 1447 cm^{-1} band for Cr($C_6H_5NH_2$)$_2$ is by about 100 cm^{-1} red-shifted, while the higher one (1529 cm^{-1}) is about 30 cm^{-1} red-shifted with the deuteration substitution. In fact, the DFT calculations provide the consistent prediction that both of the vibrational frequencies for the CH bending and CC stretching/deforming modes are red-shifted by 110 and 40 cm^{-1}, respectively, because the deuteration considerably results in the lowering of vibration frequency for the former CH modes. In addition, the calculated frequency for NH_2 scissoring modes is almost unchanged, although the mode is not observed experimentally. Therefore, the observed two IR signals of 1447 and 1529 cm^{-1} for Cr(aniline)$_2$ could be assigned to be the CH bending and ring CC stretching/deforming vibrations, respectively.

For free aniline, as shown in Figure 4, both the experimental and the simulated IR spectra display an intense NH_2 bending absorption band as compared to that of ring CC stretching/deforming vibrations. However, as mentioned above, both IR spectra for Cr($C_6H_5NH_2$)$_2$ and Cr($C_6D_5NH_2$)$_2$ complexes do not contain absorption bands for NH_2 bending vibrations predicted near 1600 cm^{-1}, and the calculated spectra also suggest a weak absorption character for the NH_2 bend. Indeed, the absence of the NH_2 bend for the complexes demonstrates that the corresponding absorption intensity is below the detection threshold (<0.0001 in absorbance) of the IRAS measurement, while a drastic enhancement of absorption intensity is observed for the CH bending and ring CC stretching/deformation motions of the phenyl rings on forming the sandwich complex. These CH bending and CC stretching/deformation modes reside in vibrations of the phenyl frameworks (π rings) and could be enhanced by charge transfer between the Cr atom and the π rings. Indeed, vibrational studies of organometallics have demonstrated that charge transfer between the transition metal and ligands works to enhance the absorption intensity for specific vibrational modes.[66,67] It is deduced that the IR intensities of the CH and CC vibrational modes might be selectively enhanced due to the charge transfer with the d−π interactions, while those for the NH-groups separated from the phenyl framework were rather unchanged.

Furthermore, selective observation of specific vibrational modes can be accounted for by the surface selection rule of IRAS; only the vibrational modes whose transition dipoles are perpendicular to the surface are active.[68,69] The dipole of the NH_2 bending vibration is parallel to the phenyl-ring plane so that the loss of the

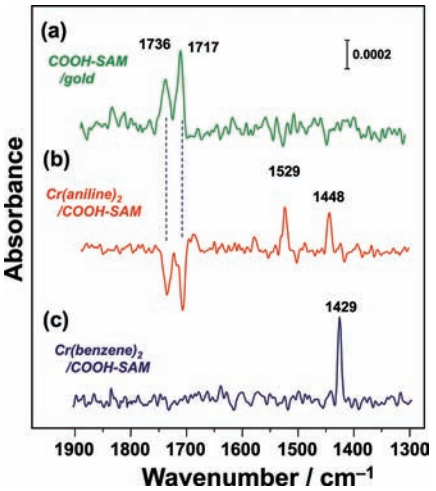

Figure 5. IRAS spectra of (a) COOH−SAM surface obtained using a clean gold surface as a background; (b) modified COOH−SAM after deposition of 2.0×10^{14} Cr(aniline)$_2$ cations at the surface temperature of 240 K obtained using unmodified COOH−SAM as a background; and (c) Cr(benzene)$_2$ complexes soft-landed on COOH−SAM.

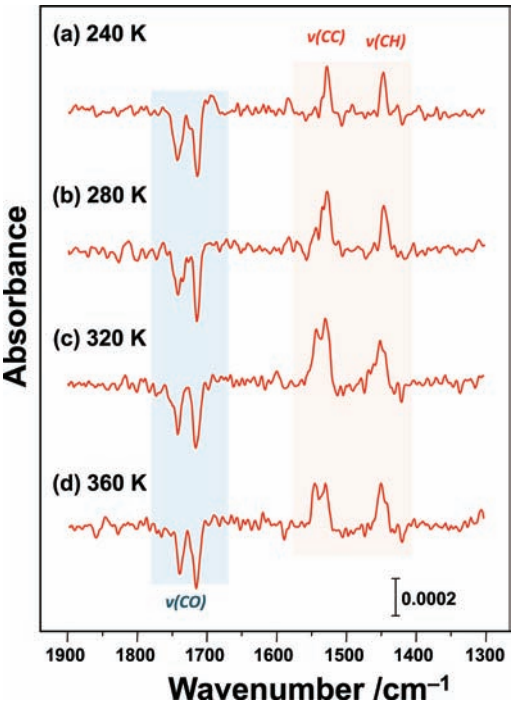

Figure 6. Temperature dependences of IRAS spectra in 240−360 K for Cr(aniline)$_2$ landed on COOH−SAM at 240 K.

NH_2 absorption might indicate that the complex is oriented on the SAM substrates with its molecular axis along the surface normal direction. However, our previous studies demonstrate that the CH−π weak hydrogen-bonding interaction between the phenyl ring and the alkyl chains of the SAM orients the sandwich complexes in such a way as to tilt their molecular axes far from the surface normal direction;[53,57] the NH_2 absorption might be allowed by this orientation. If the Cr(aniline)$_2$ sandwich complexes also involve the CH−π interaction in the SAM, the orientation should be a minor cause of a missing NH_2 bending mode.

3.2. Reactive-Landing of Cr(aniline)$_2$ on COOH−SAM. Figure 5a shows the IRAS spectrum of the COOH−SAM surface under the ultrahigh vacuum conditions with the surface temperature of 240 K. The spectrum was measured when the clean gold surface without COOH−SAM was used as a background spectrum. The characteristic bands for the free and hydrogen-bonded C═O stretching modes were observed at 1735 and 1718 cm^{-1}, respectively.[70]

Figure 5b shows the IRAS spectrum after the soft-landing of 2.0×10^{14} Cr(aniline)$_2$ cations, when the cations were landed onto COOH−SAM with the collision energy of ∼5 eV at the surface temperature of 240 K. Because the spectrum in Figure 5b was obtained by the subtraction from a background spectrum for the COOH−SAM surface before the soft-landing, a positive peak corresponds to the appearance of vibrations by newly landed species, while a negative one corresponds to the disappearance of vibrations in the COOH−SAM.

The spectrum shows that the Cr(aniline)$_2$ complexes landed on the COOH−SAM keep the sandwich formation in a neutral state after the hyperthermal depositions, because the positive peaks of 1529 and 1447 cm^{-1} are in absolute agreement with those for Cr(aniline)$_2$ complexes supported inside the CH_3−SAM matrices as shown in Figure 3. On the other hand, negative IR signals of 1736 and 1717 cm^{-1} in Figure 5b are assignable to the C═O stretching of the COOH−SAM as shown in Figure 5a. The depletions of C═O stretching peaks should be caused by structural disordering of the COOH−SAM surface, and two reasons are conceivable: (1) the orientation of the terminal carboxyl group is changed by the adsorption of Cr(aniline)$_2$ and (2) amide bonds are newly formed with the impinging clusters. Although the two are not exclusive to each other, the latter of the amide bond formation seems favorable as discussed below.

Figure 5c shows the IRAS spectrum when Cr(benzene)$_2$ cations were landed onto the COOH−SAM instead of Cr(aniline)$_2$ cations. No negative IR peaks were observed, while the positive peak of 1429 cm^{-1} could be assigned to be the CH bending vibrations of Cr(benzene)$_2$. The depletions of the IR peaks assignable to terminal carboxyl group were observed only when amine-containing complexes are landed. Therefore, the negative IR peaks are seemingly attributed to the formation of the amide bond through the reactive landing of Cr(aniline)$_2$ complexes rather than the change in the orientation of terminal carboxyl group with the adsorption of Cr(aniline)$_2$. In the hyperthermal collision event of gas-phase compounds with SAM surfaces, indeed, it has been reported that the chemical reactions take place between the projectiles and terminal groups of SAM surface,[35,57] as well as the trapping of the incoming species as they are.[48,58,59]

This explanation will be further ascertained by the surface heating and thermal desorption studies. The thermal stability of the landed Cr(aniline)$_2$ complexes at the COOH−SAM surface was evaluated by monitoring the IRAS spectra during a surface heating process. Figure 6 shows temperature dependences of the IRAS spectra for the COOH−SAM in the range of 240−360 K after 2.0×10^{14} Cr(aniline)$_2$ complexes were landed at the surface temperature of 240 K. For both the positive ν(CC) and ν(CH) and the negative ν(CO) bands, the integrated intensities are almost unchanged even after the surface is heated up to 360 K. For instance, the change in intensities for ν(CC) modes were only within 7% in 240−360 K, although the relative peak intensity was varied slightly with the surface temperature due to temperature-dependent orientation angles of polymethylene

dx.doi.org/10.1021/ja205384q |J. Am. Chem. Soc. 2011, 133, 18719–18727

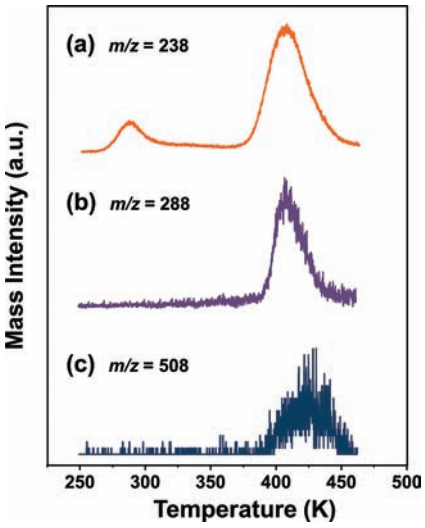

Figure 7. TPD spectra obtained for $Cr(aniline)_2$ complexes reactive-landed on COOH−SAM after deposition of 1.0×10^{14} cations at the surface temperature of 250 K with the heating rate of 3 K/s. Three kinds of desorption mass signals were mainly recorded: (a) $Cr(aniline)_2$ (238 amu), (b) 16-carboxylpentadecanethiol (288 amu), and (c) their reacted compound (508 amu).

chains forming the COOH−SAM matrix.[71] As compared to the desorption of physisorped complexes below 280 K,[59] it is evident that the $Cr(aniline)_2$ complexes landed on the COOH−SAM are firmly bound at the surface, implying that a covalent bond could be formed between the $Cr(aniline)_2$ and the SAM surface.

Although the formation of the new amide bond would provide additional IR absorption for amide I (C═O stretching, around 1800 cm^{-1}) and amide II bands (N−H bending, around 1450 cm^{-1}) in the IRAS spectrum, no amide bands were observed. This result implies that the amide bands are rendered unfavorable by the IRAS surface selection rule. Indeed, it has been reported that the surface amide groups formed by the surface reaction of alkyldiamine molecules and imidyl-ester-terminated SAM contain no absorption bands in the IRAS spectrum.[38] Furthermore, no substantial IR peak shifts for ν(CC) and ν(CH) modes were found between free and amide-bonded $Cr(aniline)_2$ complexes (in Figures 3a and 5b). In fact, our DFT calculations show that the frequency shifts obtained are only within 2 cm^{-1}, when one of the NH_2 groups in aniline ligands is converted to an amide bond with polymethylne chains.[72] In other words, chemical bond formation of the substituted amino group has less effect on the structure of phenyl frameworks in the $Cr(aniline)_2$ complexes. Therefore, the electronic structure of the functional site stemming from the d−π interaction in the complex would remain even after forming amide bonds at the SAM surface.

To characterize the thermal desorption process of the landed clusters on the COOH−SAM surface, a temperature-programmed desorption (TPD) study was conducted. Figure 8 shows the TPD spectrum for the COOH−SAM substrate after the soft-landing of mass-selected $Cr(aniline)_2$ cations (m/z = 238) with the kinetic energy of ∼5 eV at the surface temperature of 250 K. The total amount of the landed complexes was set to be 1.5×10^{14}, and the mass resolution of the spectrometer was somewhat reduced to $m/\Delta m$ = ∼120 to gain the sensitivity for large masses (>500 amu). The TPD spectra were measured by three mass channels of $Cr(aniline)_2$ (m/z = 238), 16-carboxypentadecanethiol (m/z = 288), and their reaction product (m/z = 508), the third of which corresponds to the species formed by the amide bond between the NH_2 group of $Cr(aniline)_2$ and the terminal COOH group of 16-carboxypentadecanethiol in the landing.

As shown in Figure 7a, the TPD spectrum for $Cr(aniline)_2$ exhibits two desorption bands around 280 and 410 K, showing that there are two different adsorption states of $Cr(aniline)_2$ on the COOH−SAM surface. The lower-temperature desorption around 280 K would be attributed to the physisorption states of $Cr(aniline)_2$ stabilized via interactions of COOH−π and/or COOH−NH_2 between the COOH−SAM surface and the complexes of $Cr(aniline)_2$. The higher-temperature desorption bands appeared between the substrate temperature of 380−450 K with a peak of ∼410 K. Because the desorption signals for m/z = 288 and m/z = 508 were also observed at the similar substrate temperatures of 380−450 K, it is reasonably presumed that the high-temperature desorption signals of $Cr(aniline)_2$ (m/z = 238) result from fragmentation of parent species (m/z = 508), that is, $Cr(aniline)_2$ amide bonded to a mercapto-polymethylene chain, in the electron impact ionization. In the TPD spectrum of the COOH−SAM substrate without any landing of the complexes, indeed, the desorption of 16-carboxypentadecanethiol molecules can be observed above 380 K similarly to Figure 7b, showing that the Au−S bond between 16-carboxypentadecanethiol and Au(111) dissociates. Therefore, along with the observation of the reacted compound signal (m/z = 508), the higher-temperature desorption bands in Figure 7 can be attributed to the reaction product formed by amide bond between the NH_2 group of $Cr(aniline)_2$ and the terminal COOH group of 16-carboxypentadecanethiol. In the TPD spectra, no desorption signal of $Cr(aniline)_2$ formed through the dissociation of the surface amide bond is observed before the thermal desorption of the SAM. Hence, the binding energy of the amide bond is larger than that between thiols (−SH) and gold surface (∼1.35 eV).[73]

3.3. Temperature Influence on Reactive-Landing Efficiency. After the landing at surface temperature of 240 K, some of the $Cr(aniline)_2$ cations are bound to the SAM terminal with an amide bond, while the other $Cr(aniline)_2$ are left as physisorbed species. To further discuss the reactive-landing mechanism of $Cr(aniline)_2$ to the COOH−SAM, the influence of the surface temperature of the COOH−SAM during the landing was examined on the resultant adsorption states of $Cr(aniline)_2$, for example, population change between the physisorption and amide-bond states.

Figure 8a and b shows IRAS spectra for $Cr(aniline)_2$ complexes after the landing of 1.5×10^{14} cations on the COOH−SAM with the incident energy of ∼5 eV at different surface temperatures of 200 and 250 K. The corresponding TPD spectra for $Cr(aniline)_2$ (m/z = 238) are shown in Figure 8c and d, and the ratio of integrated intensities between the two desorption states of physisorption (A) and amide bond (B) is also indicated as A/B in the figure.

For the lower-temperature landing at 200 K, the IR spectrum contains additional two bands at 1607 and 1501 cm^{-1} with the signals for $Cr(aniline)_2$ at 1529 and 1448 cm^{-1}. The additional peaks can be assigned to the vibrational modes of an aniline molecule itself. The result shows that some incident complexes dissociate into aniline molecules during the hyperthermal collisions with the COOH−SAM surface, and the fragment of aniline molecules is trapped at the low-temperature COOH−SAM surface (200 K). The two bands at 1607 and 1501 cm^{-1} for aniline fragments are missing in the IRAS at 250 K (Figure 8b),

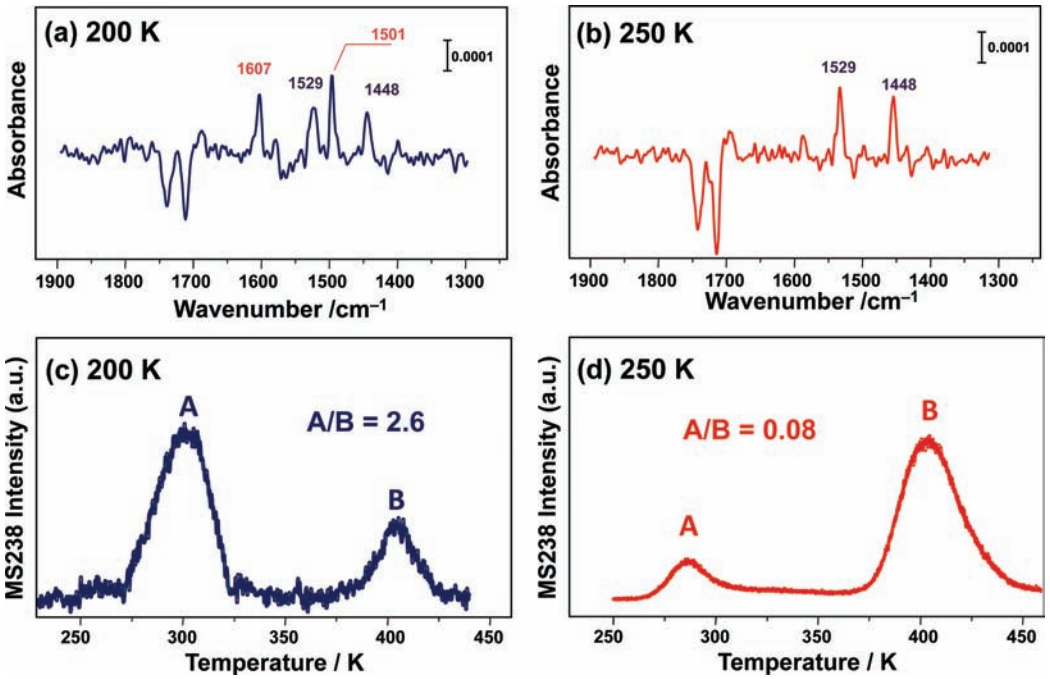

Figure 8. IRAS spectra for the $Cr(aniline)_2$ landed on the COOH−SAM at (a) 200 K and (b) 250 K, along with their corresponding TPD spectra after the landing at (c) 200 K and (d) 250 K.

because physisorped aniline molecules are desorbed above ~220 K.

When the TPD spectra are compared between 200 and 250 K in Figure 8, the intensity ratio between the physisorption state (A) and the amide-bond state (B), A/B, is significantly different: The landing at 200 K generates prominent desorption from the physisorbed state (A/B = 2.6), while the landing at 250 K does prominent desorption from the amide-bond state (A/B = 0.08). The result in Figure 8 shows that the increase in surface temperature during the landing can significantly enhance the reactive-landing efficiency for $Cr(aniline)_2$ onto the COOH−SAM.

The reactive-landing efficiency can be estimated by comparing the IR absorption intensity for the C═O stretching modes before and after the landing, under the assumption that the IR intensity for C═O stretching of COOH−SAM is not disturbed by the physisorption state. When $Cr(aniline)_2$ cations were landed onto the COOH−SAM up to 1.5×10^{14} at 200 K, the IR intensity for C═O stretching almost linearly decreases with time, and the negative intensity reaches 38% of the initial C═O absorption intensity before the landing. Because the IR light in our IRAS setup covers the whole area of the COOH−SAM (1×1 cm^2), about 1.3×10^{14} carboxyl groups were ascribed to the IR intensity for C═O stretching. The 38% of IR depletion corresponds to that 0.49×10^{14} carboxyl groups were transformed to the amide bond after the deposition of 1.5×10^{14} ions; ~33% of incoming $Cr(aniline)_2$ were bound to the SAM surface with the amide bond. On the other hand, for the landing at 250 K, the negative intensity reaches 82% of the initial C═O absorption intensity so that the reactive-landing ratio of $Cr(aniline)_2$ to the COOH−SAM is estimated to be 67%, which is about twice larger than that for the landing at 200 K.

Although an amide bond is not formed by direct reaction of amine and carboxyl group in the solution phase, gas-phase ion−surface hyperthermal collision can effectively induce novel chemical reactions that are unsuccessful in the solution phase. In the hyperthermal ion−surface collisions, projectiles undergo rapid excitation and activation through direct impact with the surface within 0.5 ps prior to thermalization at the surface.[51,74] The chemical reaction of incoming $Cr(aniline)_2$ with the COOH−SAM performed herein would be induced through such rapid excitation during the direct impact or subsequent thermalization process at the locally heated surface. If direct impact excitation plays a major role for the reaction, the efficiency of reactive-landing should increase with the collision energy between the complex and SAM, as predicted by the microcanonical reaction rate equation.[75] However, no IR absorption and TPD signals for $Cr(aniline)_2$ were observed after the landing onto the COOH−SAM, when the collision energy (incident kinetic energy) was increased to 100 eV.[72] Therefore, the collision energy was effectively dissipated not into amide-bond formation but into vibrational excitations of the projectiles[75,76] to dissociate the incoming $Cr(aniline)_2$ complexes. On the other hand, the reaction kinetics in the thermalizaiton processes should depend particularly on the temperature of the SAM surface. As mentioned above, because the efficiency for the reactive landing is sensitive to the surface temperature in this work, the result suggests the key role of the thermalization process at the surface rather than the collision processes. It is reasonably deduced that the amide bond between $Cr(aniline)_2$ and carboxyl terminates would be formed through the thermalization process at the locally heated SAM surface after the hypethermal collision event.

4. CONCLUSIONS

Gas-phase synthesized $Cr(aniline)_2$ complexes were soft-landed onto self-assembled monolayers of methyl-terminated (CH_3−SAM) and reactive-landed onto COOH−SAM at herperthermal energy of 5−20 eV. Together with DFT calculations, IRAS and TPD experiments have successfully unveiled that the sandwich form of $Cr(aniline)_2$ is embedded inside the CH_3−SAM up to

~280 K, whereas $Cr(aniline)_2$ landed onto COOH−SAM is immobilized at the surface of SAM through covalent linking of amide bonds far above room temperatures. The latter reactive-landing was enhanced with the increase in surface temperatures from 200 to 250 K at the landing, indicating that the amide bonds were formed through the thermalization process at the locally heated SAM surface in the collisions.

For the production of a novel nanostructured surface based on an understanding of the cluster−surface interaction, the mass selected cluster-beam deposition offers excellent control of the cluster size, and the precise definition of the size features has great potential applications in many fields, such as the fabrication of advanced magnetic and optical nanomaterials and semiconductor nanostructures. To achieve the preservation of not only the cluster size without any fragmentation but also the clusters' electronic and geometric properties on a surface, chemical modifications both in the functional clusters and on the surface enable us to decorate the surface with functionality of the clusters characterized by gas-phase researches, as demonstrated in this work. The strong binding of the gas-phase clusters on surfaces, while keeping the electronic properties of the functional sites by separating them from the binding site, provides high thermal stability. Hence, this method opens up a new opportunity to utilize gas-phase synthesized species for functional devices and biotechnological media in the future.

■ ASSOCIATED CONTENT

Ⓢ Supporting Information. (1) Simulated IR absorption spectra by DFT calculation for (a) free $Cr(aniline)_2$ complexes and (b) $Cr(aniline)_2$ amide bonded with polymethylene chain, (2) collision energy dependence of (a) IRAS spectra and (b) TPD spectra for the $Cr(aniline)_2$ at the collision energy of 5 and 100 eV, and (3) the full list of authors in ref 61. This material is available free of charge via the Internet at http://pubs.acs.org.

■ AUTHOR INFORMATION

Corresponding Author
nakajima@chem.keio.ac.jp

■ ACKNOWLEDGMENT

This work is partly supported by Grant-in-Aids for Scientific Research (A) (No. 19205004) and for Young Scientist (B) (No. 21750023) from the Ministry of Education, Culture, Sports, Science, and Technology and by the Science Research Promotion Fund from the Promotion and Mutual Aid Corporation for Private Schools of Japan.

■ REFERENCES

(1) Sugano, S. *Microcluster Physics*; Springer: Berlin, 1991.
(2) Haberland, H., Ed. *Clusters of Atoms and Molecules*; Springer: Berlin, 1994; Vols. I + II.
(3) Khanna, S. N., Castleman, A. W., Jr., Eds. *Quantum Phenomena in Clusters and Nanostructures*; Springer: Berlin, 2003.
(4) Knight, W. D.; Clemenger, K.; de Heer, W. A.; Saunders, W. A.; Chou, M. Y.; Cohen, M. L. *Phys. Rev. Lett.* **1984**, *52*, 2141.
(5) de Heer, W. A. *Rev. Mod. Phys.* **1993**, *65*, 611.
(6) Martin, T. P. *Phys. Rep.* **1996**, *273*, 199.
(7) Kroto, H. W.; Heath, J. R.; O'Brien, S.; Curl, C. R. F.; Smalley, R. E. *Nature* **1985**, *318*, 162.
(8) Li, J.; Li, X.; Zhai, H. J.; Wang, L. S. *Science* **2003**, *299*, 864.
(9) Guo, B. C.; Kerns, K. P.; Castleman, A. W., Jr. *Science* **1992**, *255*, 1411.
(10) Jena, P.; Castleman, A. W., Jr. *Proc. Natl. Acad. Sci. U.S.A.* **2006**, *103*, 10560.
(11) Koyasu, K.; Akutsu, M.; Mitsui, M.; Nakajima, A. *J. Am. Chem. Soc.* **2005**, *127*, 4998.
(12) Neukermans, S.; Janssens, E.; Chen, Z. F.; Silverans, R. E.; Schleyer, P. V. R.; Lievens, P. *Phys. Rev. Lett.* **2004**, *92*, 163401.
(13) Nakajima, A.; Kaya, K. *J. Phys. Chem. A* **2000**, *104*, 176.
(14) Miyajima, K.; Yabushita, S.; Knickelbein, M. B.; Nakajima, A. *J. Am. Chem. Soc.* **2007**, *129*, 8473.
(15) Yasuike, T.; Yabushita, S. *J. Phys. Chem. A* **1999**, *103*, 4533.
(16) Pendy, R.; Rao, B. K.; Jena, P.; Blanco, M. A. *J. Am. Chem. Soc.* **2001**, *123*, 3799.
(17) Kandalam, A. K.; Rao, B. K.; Jena, P.; Pandey, R. *J. Chem. Phys.* **2004**, *120*, 10414.
(18) Wang, J.; Acioli, P. H.; Jellinek, J. *J. Am. Chem. Soc.* **2005**, *127*, 2812.
(19) Kua, J.; Tomlin, K. M. *J. Phys. Chem. A* **2006**, *110*, 11988.
(20) Cleveland, C. L.; Landman, U. *Science* **1992**, *257*, 355.
(21) Bromann, K.; Félix, C.; Brune, H.; Harbich, W.; Monot, R.; Buttet, J. *Science* **1996**, *274*, 956.
(22) Bardotti, L.; Jensen, P.; Hoareau, A.; Treilleux, M.; Cabaud, B. *Phys. Rev. Lett.* **1995**, *74*, 4694.
(23) Bettac, A.; Koller, L.; Rank, V.; Meiwes-Broer, K. H. *Surf. Sci.* **1998**, *404*, 475.
(24) Goldby, I. M.; Kuipers, L.; von Issendorff, B.; Palmer, R. E. *Appl. Phys. Lett.* **1996**, *69*, 2819.
(25) Binns, C. *Surf. Sci. Rep.* **2001**, *44*, 1.
(26) Bréchignac, C.; Cahuzac, P.; Carlier, F.; Colliex, C.; Leroux, J.; Masson, A.; Yoon, B.; Landman, U. *Phys. Rev. Lett.* **2002**, *88*, 196103.
(27) Donadio, D.; Colombo, L.; Milani, P.; Benedek *Phys. Rev. Lett.* **1999**, *83*, 776.
(28) Heiz, U.; Schneider, W. D. *J. Phys. D* **2000**, *33*, R85.
(29) Jamet, M.; Wernsdorfer, W.; Thirion, C.; Mailly, D.; Dupuis, V.; Mélinon, P.; Pérez, A. *Phys. Rev. Lett.* **2001**, *86*, 4676.
(30) Kaiser, B.; Bernhardt, T. M.; Stegemann, B.; Opitz, J.; Rademann, K. *Phys. Rev. Lett.* **1999**, *83*, 2918.
(31) Palmer, R. E.; Pratontep, S.; Boyen, H.-G. *Nat. Mater.* **2003**, *2*, 443.
(32) Tong, X.; Benz, L.; Kemper, P.; Meitu, H.; Bowers, M. T.; Buratto, S. K. *J. Am. Chem. Soc.* **2005**, *127*, 13516.
(33) Gologan, B.; Green, J. R.; Alvarez, J.; Laskin, J.; Cooks, R. G. *Phys. Chem. Chem. Phys.* **2005**, *7*, 1490.
(34) Blake, T. A.; Zheng, O. Y.; Wiseman, J. M.; Takats, Z.; Guymon, A. J.; Kothari, S.; Cooks, R. G. *Anal. Chem.* **2004**, *76*, 6293.
(35) Wang, P.; Hadjar, O.; Laskin, J. *J. Am. Chem. Soc.* **2007**, *129*, 8682.
(36) Laskin, J.; Wang, P.; Hadjar, O. *Phys. Chem. Chem. Phys.* **2008**, *10*, 1079.
(37) Wang, P.; Hadjar, O.; Gassman, P. L.; Laskin, J. *Phys. Chem. Chem. Phys.* **2008**, *10*, 1512.
(38) Hu, Q. C.; Wang, P.; Gassman, P. L.; Laskin, J. *Anal. Chem.* **2009**, *81*, 7302.
(39) Meiwes-Broer, K.-H., Ed. *Metal Clusters at Surfaces: Structure, Quantum Properties, Physical Chemistry*; Springer: Berlin, 2000.
(40) Meiwes-Broer, K.-H., Ed. *Phys. Status Solidi B, Special Issue: Clusters at Surfaces* **2010**, *247*, 989.
(41) Messerli, S.; Schintke, S.; Morgenstern1, K.; Sanchez, A.; Heiz, U.; Schneider, W.-D. *Surf. Sci.* **2000**, *465*, 331.
(42) Schaub, R.; Jödicke, H.; Brunet, F.; Monot, R.; Buttet, J.; Harbich, W. *Phys. Rev. Lett.* **2001**, *86*, 3590.
(43) Sanchez, A.; Abbet, S.; Heiz, U.; Schneider, W.-D.; Hakkinen, H.; Barnett, R. N.; Landman, U. *J. Phys. Chem. A* **1999**, *103*, 9573.
(44) Yoon, B.; Häkkinen, H.; Landman, U.; Wörz, A. S.; Antonietti, J. M.; Abbet, S.; Judai, K.; Heiz, U. *Science* **2005**, *307*, 403.
(45) Kaden, W. E.; Wu, T.; Kunkel, W. A.; Anderson, S. L. *Science* **2009**, *326*, 826.

(46) Blass, P. M.; Akhter, S.; Seymour, C. M.; Lagowski, J. J.; White, J. M. *Surf. Sci.* **1989**, *217*, 85.
(47) Choi, J.; Dowben, P. A. *Surf. Sci.* **2006**, *600*, 2997.
(48) Ouyang, Z.; Takáts, Z.; Blake, T. A.; Gologan, B.; Guymon, A. J.; Wisemen, J. M.; Oliver, J. C.; Davisson, V. J.; Cooks, R. G. *Science* **2003**, *301*, 1351.
(49) Laskin, J.; Wang, P.; Hadjar, O. *J. Phys. Chem. C* **2010**, *114*, 5305.
(50) Mitsui, M.; Nagaoka, S.; Matsumoto, T.; Nakajima, A. *J. Phys. Chem. B* **2006**, *110*, 2968.
(51) Yan, T.; Isa, N.; Gibson, K. D.; Sibener, S. J.; Hase, W. L. *J. Phys. Chem. A* **2003**, *107*, 10600.
(52) Isa, N.; Gibson, K. D.; Yan, T.; Hase, W.; Sibener, S. *J. Chem. Phys.* **2004**, *120*, 2417.
(53) Nagaoka, S.; Matsumoto, T.; Okada, E.; Mitsui, M.; Nakajima, A. *J. Phys. Chem. B* **2006**, *110*, 16008.
(54) Nagaoka, S.; Matsumoto, T.; Ikemoto, K.; Mitsui, M.; Nakajima, A. *J. Am. Chem. Soc.* **2007**, *129*, 1528.
(55) Shen, J. W.; Evans, C.; Wade, N.; Cooks, R. G. *J. Am. Chem. Soc.* **1999**, *121*, 9762.
(56) Evans, C.; Wade, N.; Pepi, F.; Strossman, G.; Schuerlein, T.; Cooks, R. G. *Anal. Chem.* **2002**, *74*, 317.
(57) Hadjar, O.; Wang, P.; Futrell, J. H.; Dessiaterik, Y.; Zhu, Z.; Cowin, J. P.; Iedema, M. J.; Laskin, J. *Anal. Chem.* **2007**, *79*, 6566.
(58) Nagaoka, S.; Ikemoto, K.; Matsumoto, T.; Mitsui, M.; Nakajima, A. *J. Phys. Chem. C* **2008**, *112*, 15824.
(59) Ikemoto, K.; Nagaoka, S.; Matsumoto, T.; Mitsui, M.; Nakajima, A. *J. Phys. Chem. C* **2009**, *113*, 4476.
(60) Peng, W.-P.; Johnson, G. E.; Fortmeyer, I. C.; Wang, P.; Hadjar, O.; Cooks, R. G.; Laskin, J. *Phys. Chem. Chem. Phys.* **2011**, *13*, 267.
(61) Frisch, M. J.; et al. *Gaussian 03*, revision D.02; Gaussian, Inc.: Wallingford, CT, 2004. See the full list of authors in the Supporting Information.
(62) van Heijnsbergen, D.; von Helden, G.; Meijer, G.; Maitre, P.; Duncan, M. A. *J. Am. Chem. Soc.* **2002**, *124*, 1562.
(63) Jaeger, T. D.; van Heijnsbergen, D.; Klippenstein, S. J.; von Helden, G.; Meijer, G.; Duncan, M. A. *J. Am. Chem. Soc.* **2004**, *126*, 10981.
(64) Moore, D. V.; Oomens, J.; Eyler, J. R.; von Helden, G.; Meijer, G.; Dunbar, R. C. *J. Am. Chem. Soc.* **2005**, *127*, 7243.
(65) Parker, D. H.; Jones, M. E.; Koel, B. E. *Surf. Sci.* **1990**, *233*, 65.
(66) Nicu, V. P.; Autschbach, J.; Baerends, E. J. *Phys. Chem. Chem. Phys.* **2009**, *11*, 1526.
(67) Rodriguez, A. M. B.; Gabriesson, A.; Motevalli, M.; Matousek, P.; Towrie, M.; Sebera, J.; Zalis, S.; Vlcek, A. *J. Phys. Chem. A* **2005**, *109*, 5016.
(68) Hayden, B. E. In *Vibrational Spectroscopy of Molecules on Surface*; Yates, J. T., Jr., Modey, T. E., Eds.; Plenum Press: New York, NY, 1987; Vol. 1, Chapter 7.
(69) Iwasa, T.; Horiuchi, K.; Shikishima, M.; Noguchi, Y.; Nagaoka, S.; Nakajima, A. *J. Phys. Chem. C* **2011**, *115*, 16574.
(70) Nuzzo, R. G.; Dubois, L. H.; Allara, D. L. *J. Am. Chem. Soc.* **1990**, *112*, 558.
(71) Nagaoka, S.; Ikemoto, K.; Matsumoto, T.; Mitsui, M.; Nakajima, A. *J. Phys. Chem. C* **2008**, *112*, 6899.
(72) See the Supporting Information.
(73) Schreiber, F. *Prog. Surf. Sci.* **2000**, *65*, 151.
(74) Martinez-Núnez, E.; Rahaman, A.; Hase, W. L. *J. Phys. Chem. C* **2007**, *111*, 354.
(75) Rakov, V. S.; Deisov, E. V.; Laskin, J.; Futrell, J. H. *J. Phys. Chem. A* **2002**, *106*, 2718.
(76) Burroughs, J. A.; Wainhaus, S. B.; Hanley, L. *J. Phys. Chem.* **1994**, *98*, 10913.